The background of the slide features a photograph of a modern cable-stayed bridge spanning a body of water, likely the Rio-Antirrio Bridge in Greece. In the foreground, several palm trees are visible on a sandy beach. The sky is blue with some white clouds.

# CAST – Direct Search for Solar Axions

Markus Kuster  
for the CAST Collaboration

TU Darmstadt  
MPE Garching

The 3<sup>rd</sup> Joint ILIAS-CERN-DESY Axion-WIMPs Training Workshop

2007 June 22

**TUD**



- Direct Solar Axion Searches
- The CERN Axion Solar Telescope – CAST
- Results of Phase I and II of CAST
- Conclusions and Prospects



# The CAST Collaboration

## Canada

### University of British Columbia, Department of Physics, Vancouver

M. Hasinoff

## Croatia

### Rudjer Bošković Institute, Zagreb

K. Jakovčić, M. Krčmar, B. Lakić, A. Ljubičić

## France

### DAPNIA, CEA-Saclay, Gif-sur-Yvette

S. Aune, T. Dafni, E. Ferrer-Ribas, I. Giomataris, I. G. Irastorza

## Germany

### TU Darmstadt, Institut für Kernphysik

D. H. H. Hoffmann, M. Kuster, A. Nordt

### GSI Darmstadt

D. H. H. Hoffmann

### Universität Frankfurt, Institut für Angewandte Physik, Frankfurt

J. Jacoby

### Universität Freiburg

H. Fischer, J. Franz, F. H. Heinsius, D. Kang, K. Königsmann, J. Vogel

### MPE Garching

H. Bräuninger, M. Kuster, A. Nordt

### WHI München

R. Kotthaus, G. Lutz, G. Raffelt, P. Serpico

## Greece

### University of Patras

Y. Semertzidis, K. Zioutas

## National Center for Scientific Research “Demokritos”, Athens

G. Fanourakis, T. Geralis, K. Kousouris

## Aristotle University of Thessaloniki

C. Eleftheriadis, A. Liolios, I. Savvidis

## Hellenic Open University, Patras

C. Bourlisi, S. Tzamarias

## Russia

### Russian Academy of Science, Institute for Nuclear Research (INR), Moscow

A. Belov, S. Glinenkov

## Spain

### University of Zaragoza

B. Beltrán, J. Carmona, S. Cebrián, J. Galán, H. Gómez, I. G. Irastorza, G. Luzón, A. Morales, J. Morales, A. Ortiz, A. Rodríguez, J. Ruz, J. Villar

## Turkey

### Dogus University, Istanbul

E. Arik, S. Boydag, S. A. Cetin, O. B. Dogan, I. Hikmet

## USA

### Lawrence Livermore National Laboratory, Livermore, CA

M. Pivovaroff, R. Souflis, K. van Bibber

### University of Chicago, Enrico Fermi Institute and KICP

J. Collar, D. Miller

## Switzerland

### European Organization for Nuclear Research (CERN), Genève

D. Autiero, K. Barth, S. Borghi, M. Davenport, L. Di Lella, N. Elias, C. Lasseur, T. Ninikowski, T. Papaevangelou, A. Palacci, H. Riege, L. Stewart, L. Walkiers

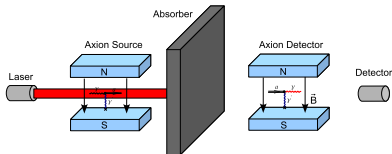




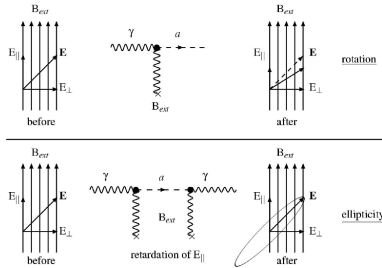
# Direct Axion Detection Techniques I

## Laser Induced Axions

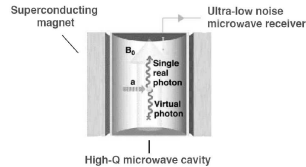
### Light Shining Through Wall



### Vacuum Properties



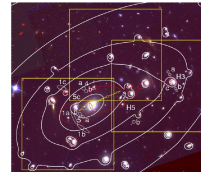
## Microwave Cavity Searches



e.g. Asztalos et al., Phys. Rev. D 69, 011101 (2004)

[astro-ph/0310042]

## Telescope Searches



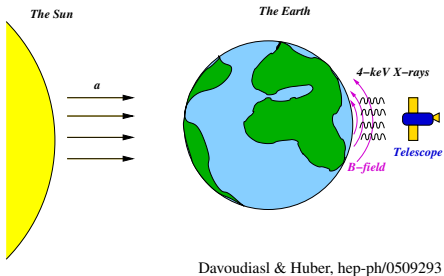
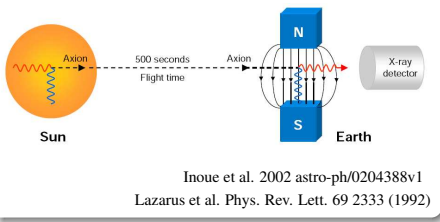
e.g. Grin et al. 2006 astro-ph/0611502v1



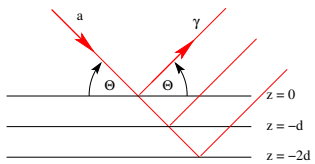
# Direct Axion Detection Techniques II – Solar Axions

## Geomagnetic Axion Conversion

### Helioscope Searches



### Bragg Diffraction

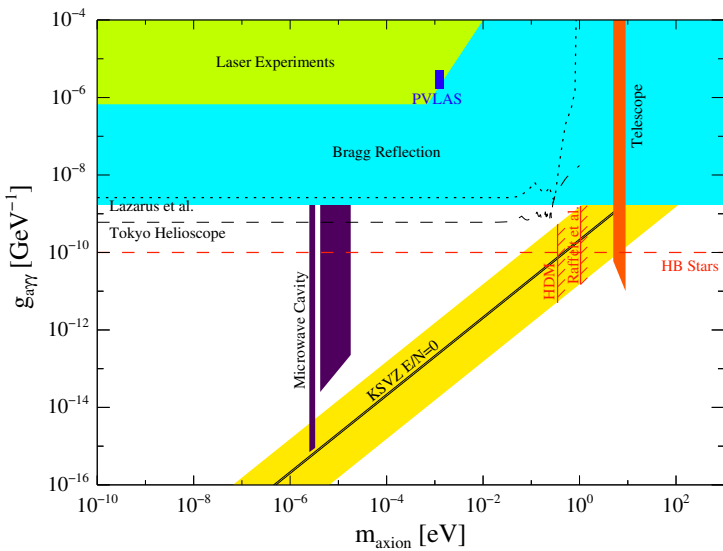


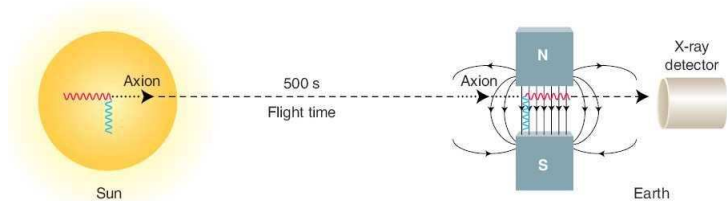
### Idea

- Axions can convert to photons in Earth's magnetic field  
⇒ Observe the Sun through the Earth
- Sensitivity  
 $g_{a\gamma\gamma} \approx 10^{-11} \text{ GeV}^{-1}$



# Limits on the Axion Parameter Space





## Principle of the Axion Helioscope P. Sikivie, Phys. Rev. Lett. 51 (1983)

- Assumption: Axions are produced via Primakoff effect in the sun
- Point a strong magnetic field towards the sun to **convert axions back to X-ray photons**
- Use background optimized X-ray detectors to **observe the X-rays**

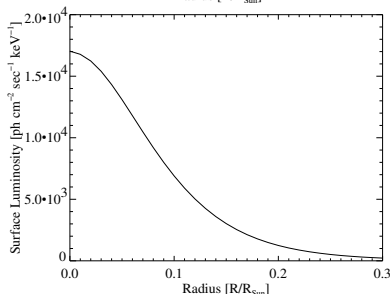
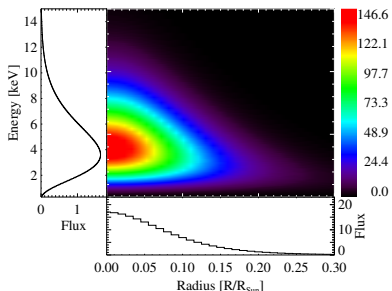
## Advantages

- ➊ Axion detection essentially assumption-free and model-independent
- ➋ Covers a broad-band mass range  $m_a \approx 0\text{--}1.2\text{ eV}$
- ➌ Observe other celestial objects

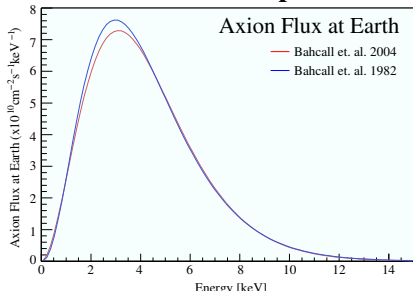


# Solar Axion Model

## Axion Surface Luminosity



## Differential Axion Spectrum



Mean Axion Energy:  $\langle E \rangle = 4.2 \text{ keV}$

Axion Luminosity:

$$L_a = g_{10}^2 \cdot 1.85 \times 10^{-3} L_{\odot}$$

Axion Flux:

$$\Phi_a = g_{10}^2 \cdot 3.75 \times 10^{11} \text{ cm}^{-2} \text{ s}^{-1}$$

Provided by P. Serpico & G. Raffelt

Based on the standard solar model BP2004 (Bahcall et al., 2004)



# Previous Helioscope Implementations

## BNL Helioscope 1992

### Experimental Parameters

- Magnet  $B = 2.2 \text{ T}$   $L \approx 1.8 \text{ m}$
- Mounted fix, 15 min observation time during sunset
- Proportional counter

Lazarus et al. Phys. Rev. Lett. 69 2333 (1992)

### Results (95% C.L.)

$$m_a < 0.03 \text{ eV}$$

$$g_{a\gamma\gamma} < 3.6 \times 10^{-9} \text{ GeV}^{-1}$$

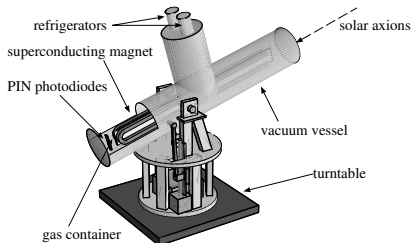
$$g_{a\gamma\gamma} < 6.0 \times 10^{-10} \text{ GeV}^{-1}$$

$$0.03 \text{ eV} < m_a < 0.11 \text{ eV}$$

$$g_{a\gamma\gamma} < 7.7 \times 10^{-9} \text{ GeV}^{-1}$$

$$g_{a\gamma\gamma} < 6.8 - 10.9 \times 10^{-9} \text{ GeV}^{-1}$$

## Tokyo Helioscope 1997-2000



Inoue et al. 2002 astro-ph/0204388v1

### Experimental Parameters

- Magnet  $B = 4 \text{ T}$   $L = 2.3 \text{ m}$
- Sky coverage  
Ra  $360^\circ$  Dec  $\pm 28^\circ$   
 $\Rightarrow$  24h observation time
- PIN-diodes



# How to Build an Axion Helioscope

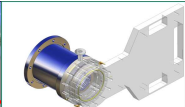
**ABRIXAS Mirror System**



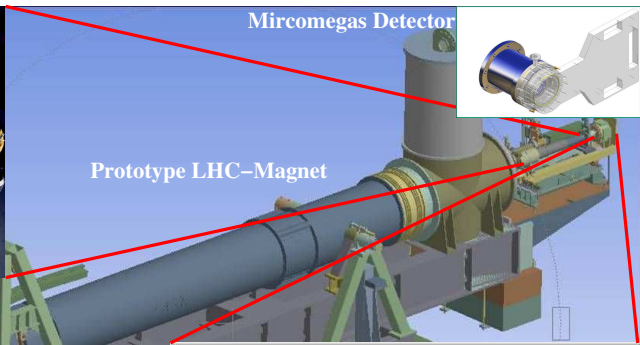
**Time Projection Chamber**



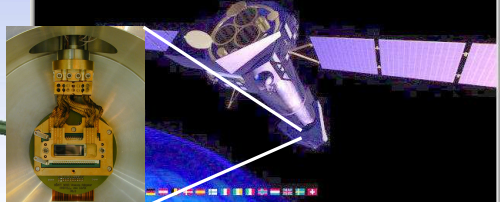
**Mircomegas Detector**

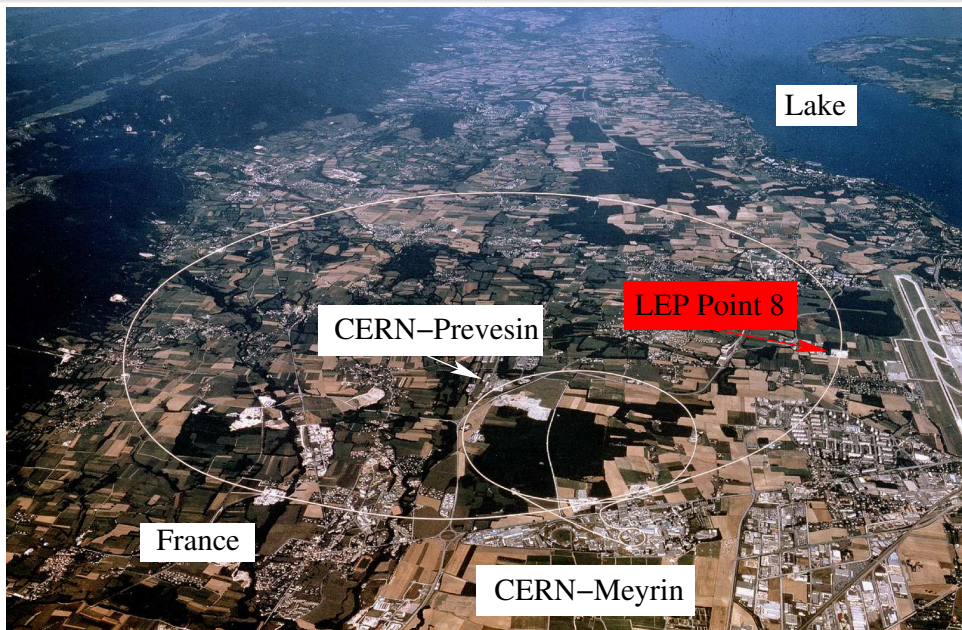


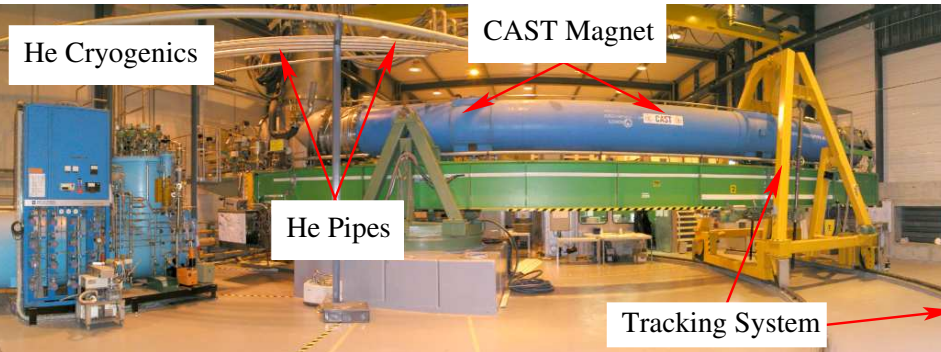
**Prototype LHC-Magnet**



**XMM-Newton EPIC-pn Detector**







## Prototype LHC magnet

$$B = 9.0 \text{ T} \quad l = 9.26 \text{ m}$$

$$T = 1.8 \text{ K} \quad m \approx 30 \text{ t}$$

## Tracking system

$$H = -8^\circ \dots 8^\circ \quad Az = 40^\circ \dots 140^\circ$$

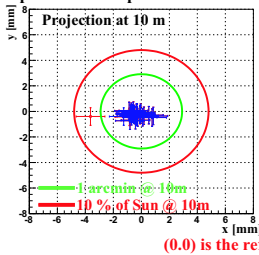
⇒ 1.5 h observation time during sun rise and sun set ( $\approx 46$  days/year)



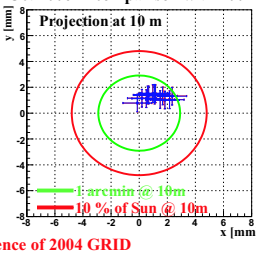
# GRID Measurements

## Verification 2002/04/06

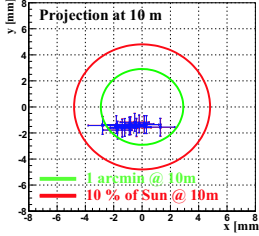
Apr 2006 in comparison with 2004



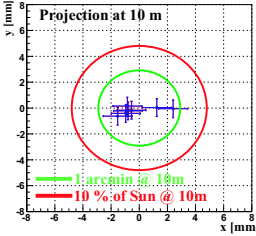
Oct 2006 in comparison with 2004



2004 in comparison with 2002

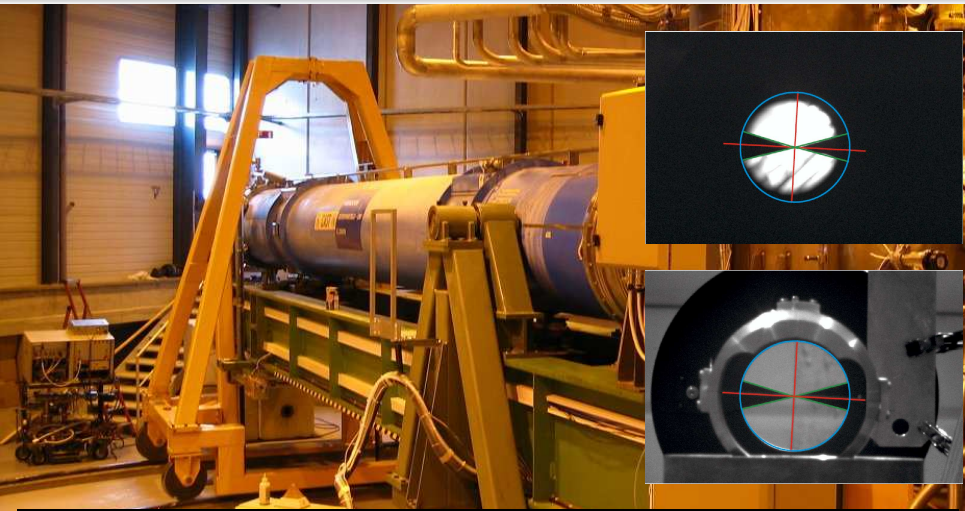


2006 in comparison with 2002



- Regular verification of the pointing precision of the tracking system
- No change observed since 2004
- Small shift with respect to 2002 grid reference  
⇒ has been corrected

Magnet points to the Sun with required precision !



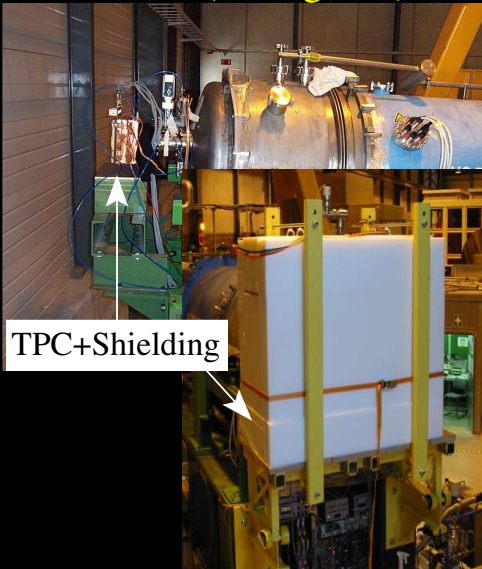
In March & September we can observe the Sun with an optical telescope.

**CAST tracks the Sun with the required precision !**

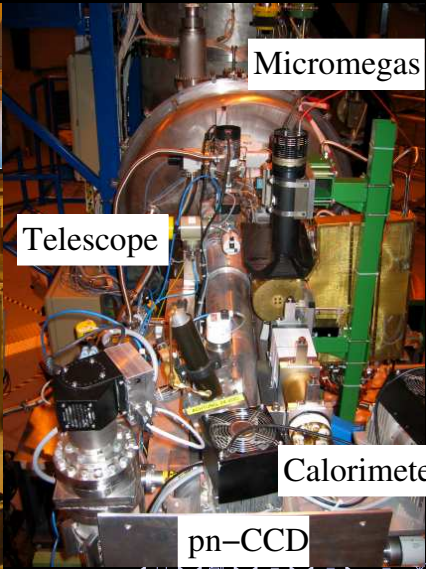


# The X-ray Detectors

East-side (setting Sun)



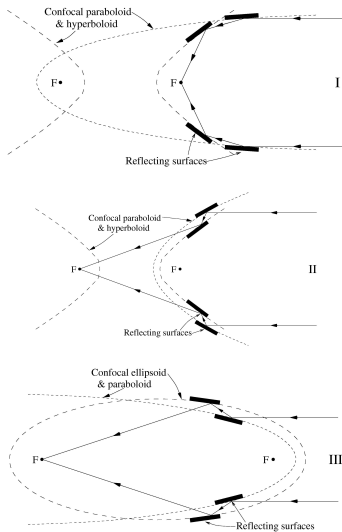
West-side (rising Sun)





# Wolter X-ray Optics

## Wolter Designs



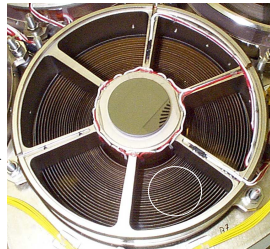
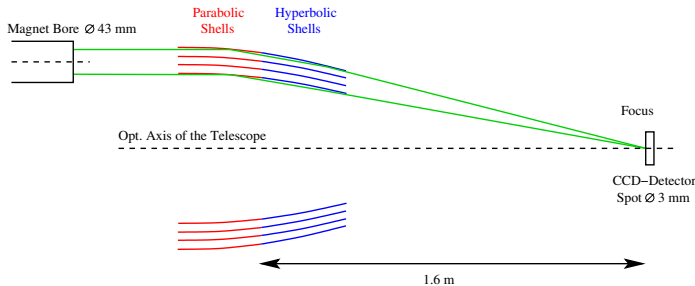
## General Properties

- Basic principle  
Total reflection for  $\Theta < \Theta_c$
- Snell's law for critical angle  $\Theta_c$   
 $\cos(\Theta_c) = n \implies \Theta_c = 2\delta$   
Far from absorption edges  
$$\Theta_c^2 = \pi \lambda^2 r_0 N_e$$
  
 $r_0$  electron radius,  $N_e$  electron density
- Basic relations  
$$\Theta_c \propto \lambda \propto 1/E_\gamma$$
  
$$\Theta_c \propto \sqrt{N_e} \simeq A$$
  
 $\implies$  High Z materials are better reflectors

Most popular Gold



# The X-ray Telescope of CAST



Wolter I type grazing incident optics (prototype for ABRIXAS mission):

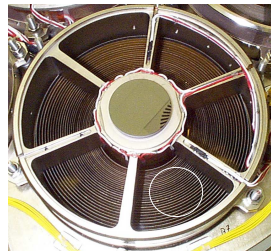
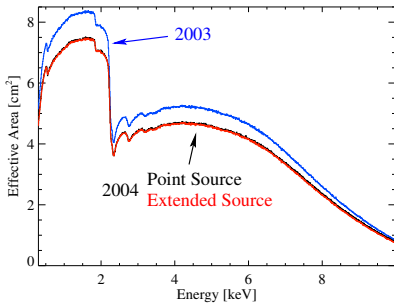
- 27 nested gold coated nickel shells, on-axis resolution  $\approx 43$  arcsec
- Telescope aperture 16 cm, used for CAST 43 mm
- Only one sector of the full aperture is used for CAST

$\varnothing 43$  mm (LHC Magnet aperture)  $\implies \varnothing 3$  mm (spot of the sun)

Significantly improves the signal to background ratio !



# The X-ray Telescope of CAST



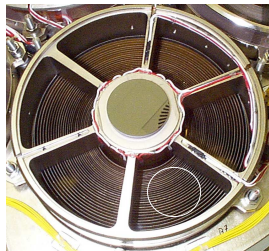
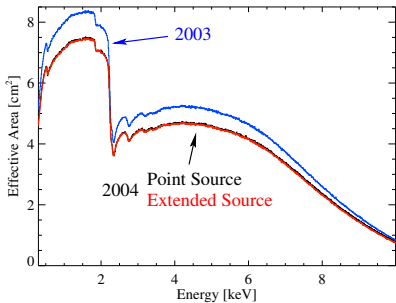
Wolter I type grazing incident optics (prototype for ABRIXAS mission):

- 27 nested gold coated nickel shells, on-axis resolution  $\approx 43$  arcsec
- Telescope aperture 16 cm, used for CAST 43 mm
- Only one sector of the full aperture is used for CAST

$\varnothing 43$  mm (LHC Magnet aperture)  $\implies \varnothing 3$  mm (spot of the sun)  
Significantly improves the signal to background ratio !



# The X-ray Telescope of CAST



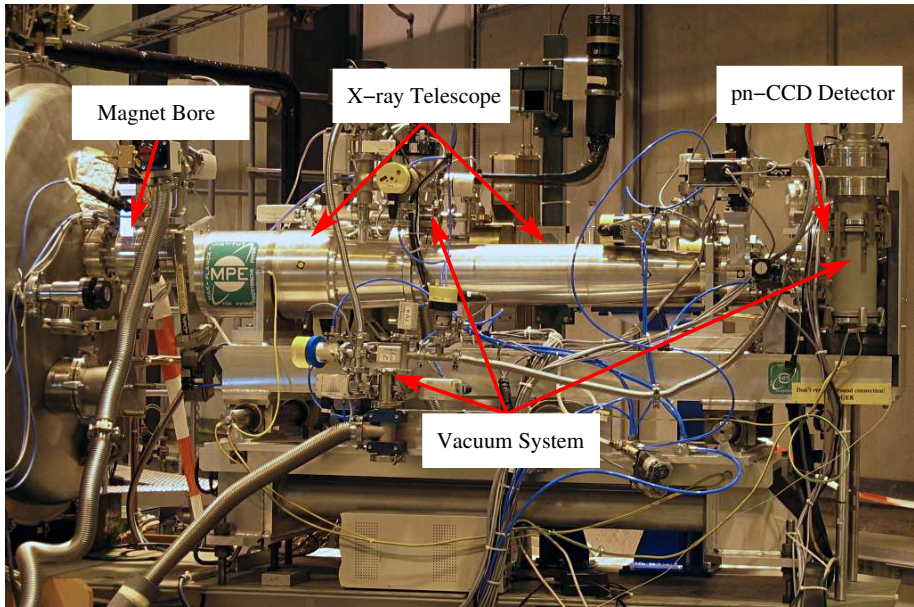
Wolter I type grazing incident optics (prototype for ABRIXAS mission):

- 27 nested gold coated nickel shells, on-axis resolution  $\approx 43$  arcsec
- Telescope aperture 16 cm, used for CAST 43 mm
- Only one sector of the full aperture is used for CAST

See following presentation by R. Soufli on X-ray optics !

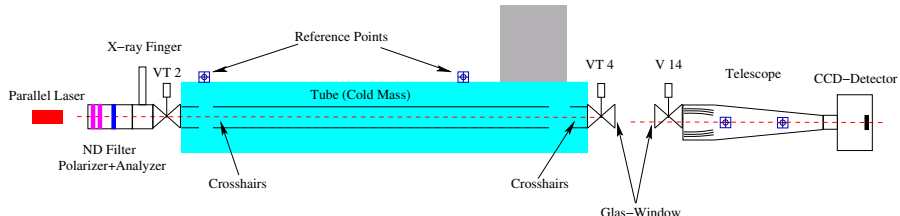


# The X-ray Telescope@CAST

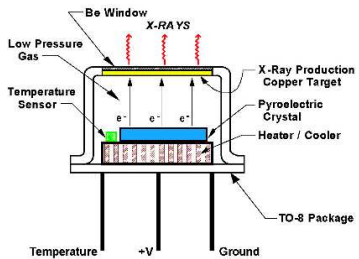




# Telescope Alignment



## X-ray Finger



## Alignment Procedure

- Use parallel laser beam to align the bore to the telescope.
- Use X-ray source to check the stability of the system.
- For both cases observe the spot on the CCD under different conditions !



## Phase I – Magnet bore evacuated

## Conversion Probability

$$P_{a \rightarrow \gamma} \propto (BL g_{a\gamma\gamma})^2 \cdot \frac{\sin^2(qL/2)}{(qL)^2} \text{ with } q = \frac{m_a^2}{2E_a}$$

For coherence:  $qL \ll 1$  (axion and photon field are in phase)

⇒ Sensitivity limit for CAST Phase I  $m_a \approx 0.02 \text{ eV}$

## Expected Count Rate (X-ray Telescope)

$$N_\gamma = \int \frac{d\Phi_a}{dE_a} P_{a \rightarrow \gamma} \epsilon t dE$$

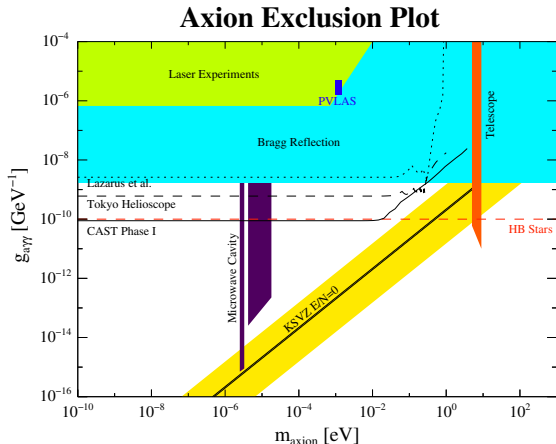
$$\Phi_\gamma \approx 1.81 g_{10}^4 \text{ counts day}^{-1}$$



# Results CAST Phase I – 2002 till 2004

## Summary

- No signal detected
- Improved CAST 2003 limit
- CAST improves previous direct experimental limits by a factor of 7
- CAST improves best astrophysical limit from HB stars



Upper limit on  $g_{a\gamma\gamma}$  for  $m_a \lesssim 0.02$  eV:

$$g_{a\gamma\gamma}(95\%) \leq 0.88 \times 10^{-10} \text{ GeV}^{-1}$$



Phase II – Magnet bore filled with buffer gas ( $^4\text{He}/^3\text{He}$ )

## Conversion Probability

$$P_{a \rightarrow \gamma} = \left( \frac{B g_a \gamma \gamma}{2} \right)^2 \frac{1}{q^2 + \Gamma^2/4} [1 + e^{-\Gamma L} - 2e^{-\Gamma L/2} \cos(qL)]$$

Absorption coefficient:  $\Gamma$

⇒ photon acquires an effective mass

$$q = \left| \frac{m_\gamma^2 - m_a^2}{2E_a} \right| \quad m_{\gamma, \text{eff}} \approx \sqrt{\frac{4\pi\alpha n_e}{m_e}} = 28.9 \sqrt{\frac{Z}{A} \rho} \approx \sqrt{0.02 \frac{P[\text{mbar}]}{T[\text{K}]}} [\text{eV}]$$

Coherence for:  $\sqrt{m_\gamma^2 - \frac{2\pi E_a}{L}} < m_a < \sqrt{m_\gamma^2 + \frac{2\pi E_a}{L}}$

Fill magnet pipes with gas ⇒ coherence restored

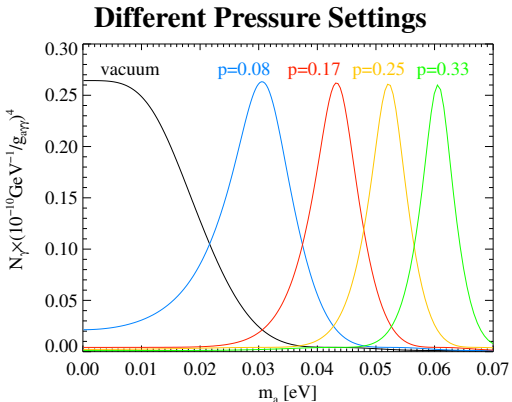
⇒ Enter axion parameter range favored by theoretical models  $m_a > 0.02 \text{ eV}$



Possible buffer gases

$^4\text{He}$  or  $^3\text{He}$

( $p_{\text{vap}} = 16/140 \text{ mbar} @ 1.8 \text{ K}$ )



Systematically change pressure  $\Rightarrow$  scan mass range  $m_a > 0.02 \text{ eV}$

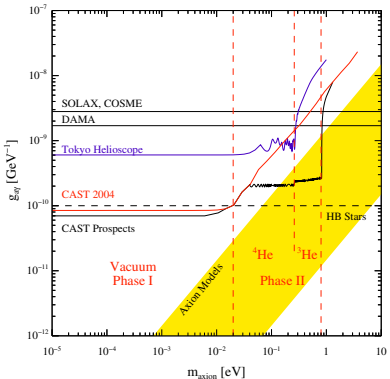
- $^4\text{He}$ :  $\approx 160$  pressure steps  $0 \leq p \leq 13 \text{ mbar}$   $m_a \leq 0.4 \text{ eV}$
- $^3\text{He}$ :  $\approx 660$  pressure steps  $13 < p \lesssim 135 \text{ mbar}$   $m_a \leq 1.2 \text{ eV}$

$\Rightarrow$  Allows to scan axion masses  $0.02 \text{ eV} \leq m_a \leq 1.12 \text{ eV}$



## CAST Phase I/II

Possible buffer gases  
 ${}^4\text{He}$  or  ${}^3\text{He}$   
( $p_{\text{vap}} = 16/140 \text{ mbar} @ 1.8 \text{ K}$ )



Systematically change pressure  $\implies$  scan mass range  $m_a > 0.02 \text{ eV}$

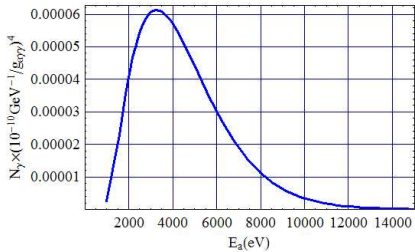
- ${}^4\text{He}$ :  $\approx 160$  pressure steps  $0 \leq p \leq 13 \text{ mbar}$   $m_a \leq 0.4 \text{ eV}$
- ${}^3\text{He}$ :  $\approx 660$  pressure steps  $13 < p \lesssim 135 \text{ mbar}$   $m_a \leq 1.2 \text{ eV}$

$\implies$  Allows to scan axion masses  $0.02 \text{ eV} \leq m_a \leq 1.12 \text{ eV}$

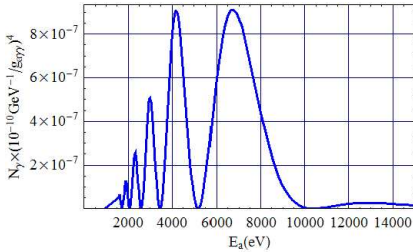


# CAST Phase II – Off Resonance Spectrum

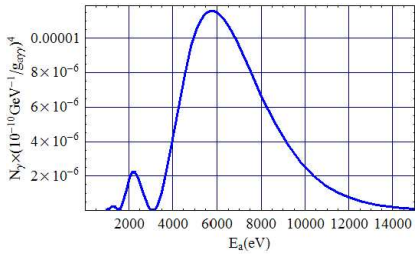
On Resonance



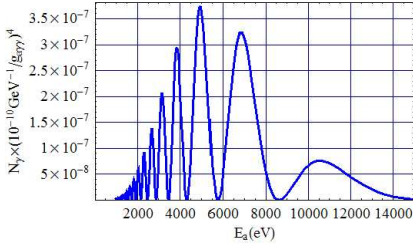
Off Resonance  $\Delta m = 0.007 \text{ eV}$



Off Resonance  $\Delta m = 0.002 \text{ eV}$



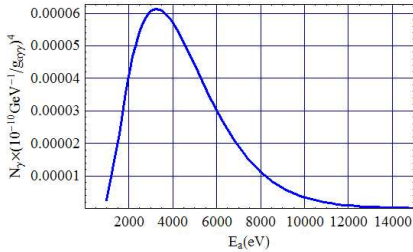
Off Resonance  $\Delta m = 0.011 \text{ eV}$



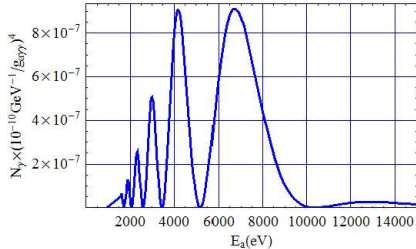


# CAST Phase II – Off Resonance Spectrum

On Resonance



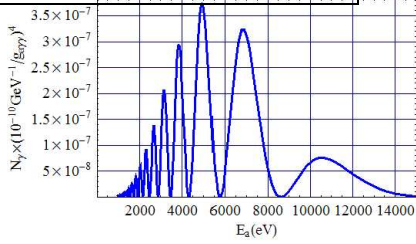
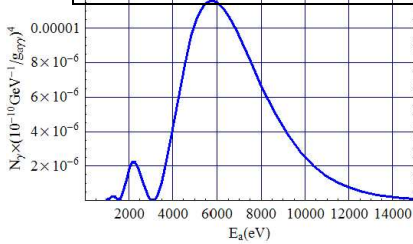
Off Resonance  $\Delta m = 0.007 \text{ eV}$

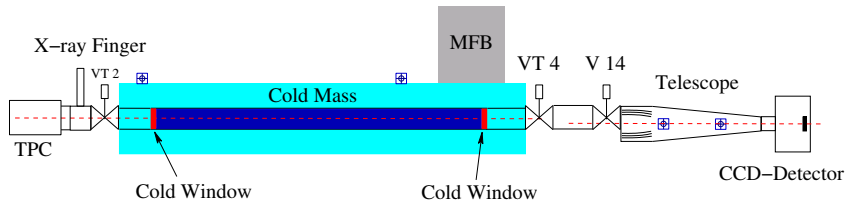


Off

**Signature to identify an axion signal !**

eV



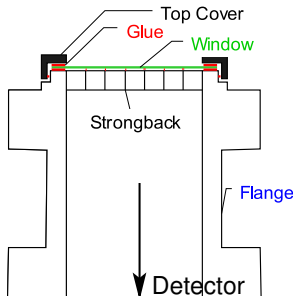


## Cold Windows/He-Gas System

- Cold windows (installed)/He-Gas System
- $^4\text{He}$  gas system (in operation 2005–2006)  
max.  $^4\text{He}$  pressure  $\approx 13.4 \text{ mbar} \implies m_a \approx 0.39 \text{ eV}$
- $^3\text{He}$  gas system installation in progress since start of 2007  
max.  $^3\text{He}$  pressure  $\approx 136 \text{ mbar} \implies m_a \approx 1.2 \text{ eV}$



## Prototype Cold Window 2005



### Technical Requirements

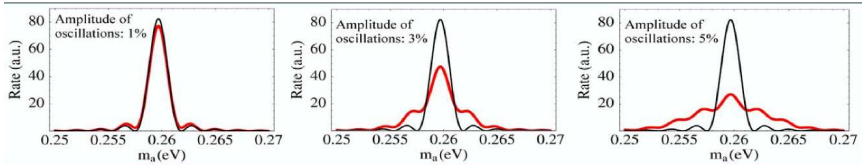
- High transmissivity at 1–7 keV
- Minimum He leak rate  
 $q_{^4\text{He}} < 10^{-8} \text{ mbar l/s}$  at 1.8 K
- Transparent in the optical  $\Rightarrow$  alignment of the telescope
- Survive a “Quench” ( $\approx 1 \text{ bar}$ )

### Design

- Polypropylene 15  $\mu\text{m}$
- Electro-eroded strong-back
- Tests and Qualification:  
CERN Cryolab



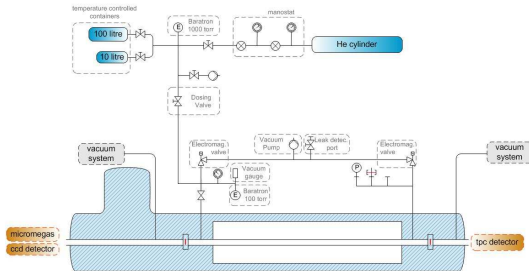
## Expected Photon Signal Depending on Oscillation Amplitude



## Pressure Oscillations in the Cold Bore

- Triggered by temperature gradient in the connection cold bore → outside world for  $p > 2$  mbar
- Frequency  $f = 3.7$  Hz with 6% amplitude
  - ⇒ 3.4% density fluctuation ( $\Delta p/p$ )
  - ⇒ Significant loss in sensitivity !

Installed dampers ⇒ problem solved !



## <sup>4</sup>He Operation

- System operated 2005 – 2006  $\Rightarrow$  well understood
- Thermo-acoustic oscillations eliminated
- Windows regularly backed out  $\Rightarrow$  avoid contamination
- Window flanges heated to 120 K  $\Rightarrow$  avoid cryopumped gases to contaminate windows

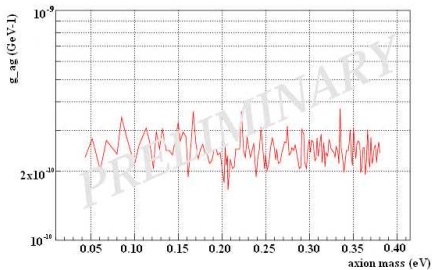


# Phase II Results ${}^4\text{He}$ – MM

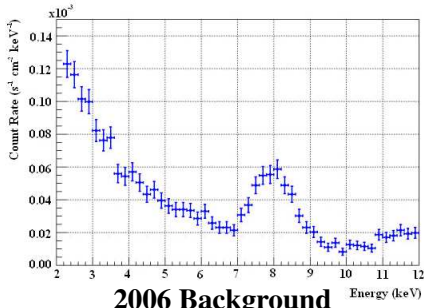
## Micromegas ${}^4\text{He}$ Data Taking

- Completed 145 density steps (277 h tracking data, 3306 h background data)
- New improved detector installed for  ${}^4\text{He}$  data taking

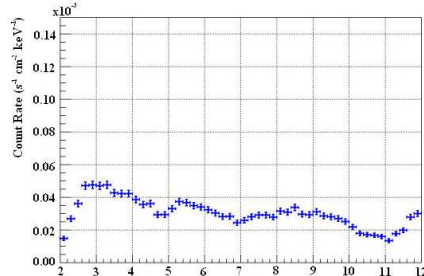
## Preliminary Result ${}^4\text{He}$



## 2005 Background



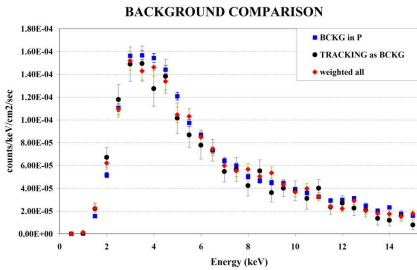
## 2006 Background



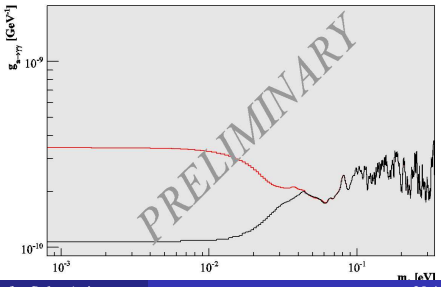
## TPC $^4\text{He}$ Data Taking

- Completed 155 density steps (501 h tracking data, 3000 h background data)
- Improved shielding
- Stable performance (no background variation depending on magnet orientation)

## 2006 Background



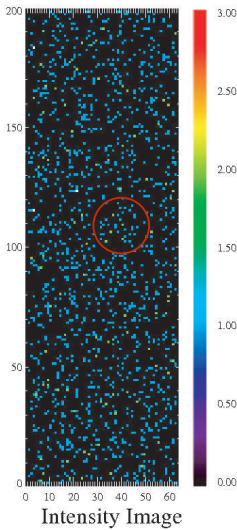
## Preliminary Result $^4\text{He}$



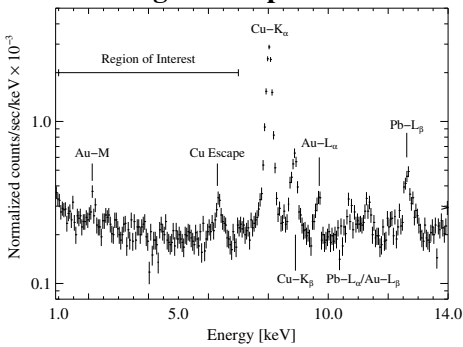


# Phase II Results ${}^4\text{He}$ –X-ray Telescope

## Background Data



## Background Spectrum



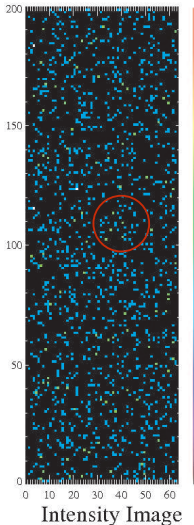
## Performance

- Background  $8.54 \pm 0.17 \times 10^{-5} \text{ counts cm}^{-2} \text{ s}^{-1} \text{ keV}^{-1}$
- Single pressure/mass step  $0.24 \pm 0.04 \text{ counts tracking}^{-1}$

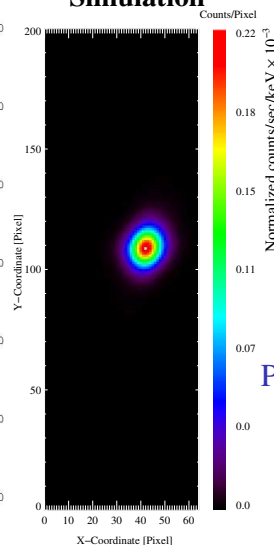


# Phase II Results $^4\text{He}$ –X-ray Telescope

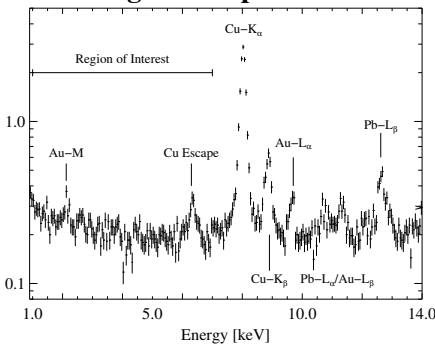
## Background Data



## Simulation



## Background Spectrum



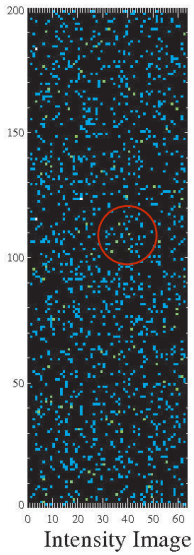
## Performance

- Background  $8.54 \pm 0.17 \times 10^{-5} \text{ counts cm}^{-2} \text{ s}^{-1} \text{ keV}^{-1}$
- Single pressure/mass step  $0.24 \pm 0.04 \text{ counts tracking}^{-1}$

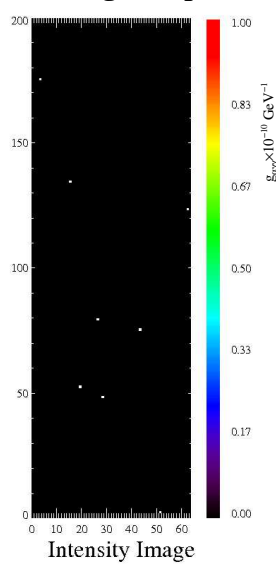


# Phase II Results $^4\text{He}$ –X-ray Telescope

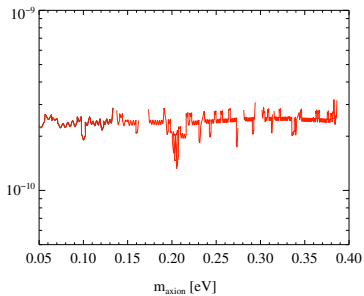
All Data



Single Step



Preliminary Result  $^4\text{He}$

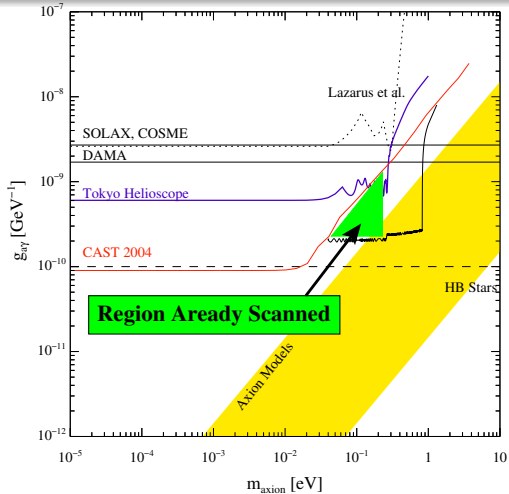


- 144 density steps 300 h high quality data
- Spot location continuously monitored

No signal detected !



# Status of Phase II



**$^4\text{He}$  runs of Phase II finished ! No signal detected !**

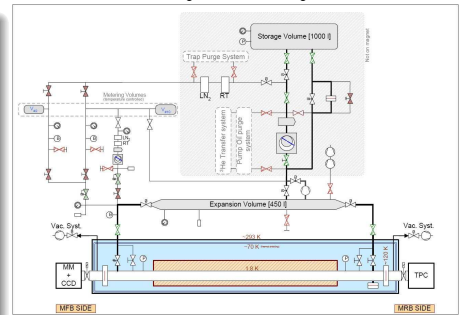


# $^3\text{He}$ Gas System – Cryolab CERN

## Requirements

- Safety against loss of  $^3\text{He}$ /release only to storage vessel
- Metering of the amount of  $^3\text{He}$  in the magnet bores (100 ppm) + reproducibility
- Absence of thermo-acoustic oscillations
- Protection of the thin X-ray windows during a quench
- Remote data logging of the state of the gas system
- “Stepping”/“Ramping”-Mode

## $^3\text{He}$ System Layout



Technical Design Report  
(CERN-SPSC-2006-029)

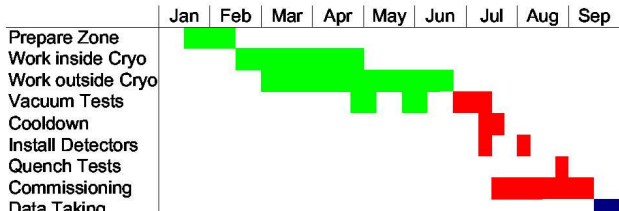
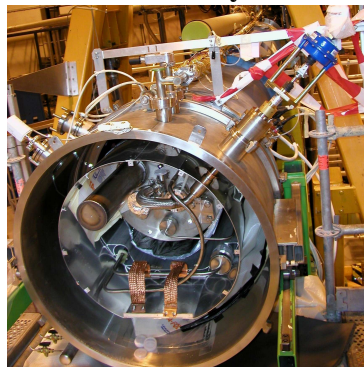
Successful review October 2006  
⇒ started manufacturing and integration



# <sup>3</sup>He Gas System – Status

- Cold window development
- 3D modeling of new components (very limited space), e.g. cryogenic valves, rupture disk, ...
- Inside cryostat: welding, cutting, installation of new components
- Design and manufacturing of large storage vessels
- PLC for gas system operation and control

## Inside the Cryostat





# New Micromegas Line 2007 – Overview

## X-ray Concentrator

- Focal length 1.3 m
- 14 Iridium coated plastic shells
- Throughput  $\approx 36\%$
- 3 mm spot diameter (100 $\times$  background reduction)

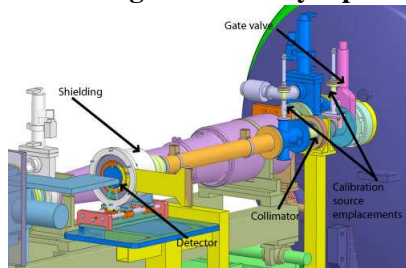
## Optimized Shielding

- Copper, Lead, Cadmium and Polyethylen + N<sub>2</sub> flux
- Expected background reduction factor 4

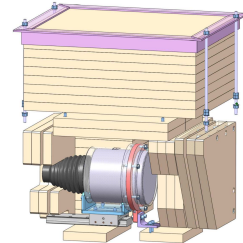
## Detector Gas

- Change Argon to Xenon  
 $\implies$  10% gain in conversion

## Micromegas with X-ray Optics



## PE Shield





## CAST and Low Energy Axions

Potential new field beyond QCD axions

Solar magnetic fields  $B \implies$  ignored so far ( $B_{\text{sunspots}} < 0.5 \text{ T}$ )

- Sun as a strong source of low energy axions (visible/UV)  
 $\implies$  Opportunity: next solar maximum
- Mechanism behind outstanding problems in solar physics ?  
Solar corona problem  
 $B^2$  dependence of X-ray flux
- CAST as complementary experiment to laboratory-based experiments

Analysis of CAST Phase I data is in progress.  
See presentations of K. Zioutas/S. Solanki



# Conclusions

- CAST Phase I provides best laboratory based upper limit for  $m_a < 0.02 \text{ eV}$

$$g_{a\gamma\gamma} < 8.8 \times 10^{-11} \text{ GeV}^{-1}$$

which is comparable to the best astrophysical limit

- Phase II  ${}^4\text{He}$  data taking finished in December 2006
  - ⇒ no signal detected
  - ⇒ CAST will reach the predicted sensitivity for  $m_a < 0.4 \text{ eV}$
- Preparation for  ${}^3\text{He}$  measurements are in progress
  - expect first data in September this year
- Request for extension to run in 2008–2010
  - Main goal: Cover mass range up to  $m_a \approx 1.16 \text{ eV}$

Keep fingers crossed that we will experience the opposite to PVLAS !  
A signal appears ...

**Thanks to All Collaboration Members !!!**